JACS
JOURNAL OF THE AMERICAN CHEMICAL SOCIETY
Cite This: J. Am. Chem. Soc. 2019, 141, 3404−3408
Communication
pubs.acs.org/JACS

Superconductivity in $Bi_3O_2S_2Cl$ with Bi−Cl Planar Layers

Bin-Bin Ruan,[†,‡] Kang Zhao,[†,‡] Qing-Ge Mu,[†,‡] Bo-Jin Pan,[†,‡] Tong Liu,[†,‡] Huai-Xin Yang,[†,‡,§,¶] Jian-Qi Li,[†,‡,§,¶] Gen-Fu Chen,[†,‡,§,¶] and Zhi-An Ren*[,†,‡,§,¶]

[†]Institute of Physics and Beijing National Laboratory for Condensed Matter Physics, Chinese Academy of Sciences, Beijing 100190, People's Republic of China

[‡]School of Physical Sciences, University of Chinese Academy of Sciences, Beijing 100049, People's Republic of China

[§]Collaborative Innovation Center of Quantum Matter, Beijing 100190, People's Republic of China

[¶]Songshan Lake Materials Laboratory, Dongguan, Guangdong 523808, People's Republic of China

Supporting Information

ABSTRACT: A quaternary compound $Bi_3O_2S_2Cl$, which consists of novel $[BiS_2Cl]^{2-}$ layers, is reported. It adopts a layered structure of the space group *I*4/*mmm* (No. 139) with lattice parameters: a = 3.927(1) Å, c = 21.720(5) Å. In this compound, bismuth and chlorine atoms form an infinite planar layer, which is unique among the bismuth halides. Superconductivity is observed in both polycrystals and single crystals, and is significantly enhanced in the samples prepared with less sulfur or at higher temperatures. By tuning the content of sulfur, $Bi_3O_2S_2Cl$ can be converted from a semiconductor into a superconductor. The superconducting critical temperature ranges from 2.6 to 3.5 K. Our discovery of the $[BiS_2Cl]^{2-}$ layer opens another door in searching for the bismuth compounds with novel physical properties.

Bismuth chalcogenides of layered structure have been intensively studied in recent years. For instance, Bi_2Te_3 is one of the best performing thermoelectric materials at room temperature.[1−3] More interests were attracted after Bi_2Se_3 and Bi_2Te_3 were identified as topological insulators.[4,5] Recently, superconductivity was discovered in the $BiCh_2$-based compounds (Ch = S or Se), such as $Bi_4O_4S_3$, $Bi_3O_2S_3$, $REO_{1-x}F_xBiS_2$ (RE = La, Ce, Pr, Nd, Yb), $La_{1-x}M_xOBiS_2$ (M = Ti, Zr, Hf, Th), $Sr_{1-x}La_xFBiS_2$, and $LaO_{1-x}F_xBiSe_2$.[6−15] These compounds are of layered structures where superconductivity was introduced by carrier doping in semiconducting parent compounds, which is quite similar to the cases in the cuprates and iron-based superconductors.[16,17]

All of these superconducting $BiCh_2$-based compounds consist of $[Bi_2Ch_4]^{2-}$ layers separated by other stacking layers, which are basically fluorite-type layers such as $[Bi_2O_2]^{2+}$, $[RE_2O_2]^{2+}$, $[Sr_2F_2]^{2+}$, or the more complicated $[Eu_3F_4]^{2+}$ layers.[6,8,9,18] Large anions, say $[SO_4]^{2-}$ in $Bi_4O_4S_3$ and S_2^{2-} in $Bi_3O_2S_3$, can also be inserted between the layers.[6,7] The tolerance of anion incorporation implies that we might insert other kinds of anions, like halogens into the lattice to form new structures.

The physical properties of the bismuth halides/oxyhalides, on the other hand, were not much studied until recent years when some of them were found to have outstanding photochemical performances. For instance, BiOCl is an efficient photocatalyst to decompose organic pollutants.[19,20] More recently, the bismuth halide perovskites $Cs_3Bi_2X_9$ (X = Cl, Br, or I) were found to have outstanding photoluminescence properties and hence potential applications in solar cells.[21−23] Bismuth halides usually adopt three-dimensional structures as in $BiCl_3$, Bi_6Cl_7, and Bi_7Cl_{10},[24−26] while bismuth and halogens form quasi-one-dimensional chains in the cases of BiBr and BiI.[27,28] In many bismuth halides such as BiI_3, Cs_3BiCl_6, or $Cs_3Bi_2X_9$, the bismuth and halogen atoms form octahedra complexes of $[BiX_6]^{3-}$, which are linked with each other to form the perovskite phases.[21,29,30] However, none of these halides consists of infinite Bi−X planar layers.

BiOCl adopts a layered tetragonal crystal structure in which the $[Bi_2O_2]^{2+}$ layers are separated by the Cl^- anions.[31] Due to the structural similarity with $LaOBiS_2$, one can expect it to be an ideal source to introduce halogens into the $BiCh_2$-based compounds. Here we report the introduction of Cl^- anions into the Bi−O−S system by using BiOCl, which resulted in a layered compound $Bi_3O_2S_2Cl$. Instead of being inserted between the $[Bi_2S_4]^{2-}$ and $[Bi_2O_2]^{2+}$ layers, the Cl atoms form a novel $[BiS_2Cl]^{2-}$ layer. To our knowledge, it is the first compound with this kind of layer. Superconductivity was observed in $Bi_3O_2S_2Cl$, which was introduced by carrier doping caused by the sulfur vacancies.

Figure 1 shows the powder X-ray diffraction (XRD) pattern of polycrystalline $Bi_3O_2S_2Cl$. Except for tiny impurities, all the reflection peaks can be attributed to a new compound $Bi_3O_2S_2Cl$, which crystallizes in the space group of *I*4/*mmm* (No. 139) with the lattice parameters of a = 3.927(1) Å, c = 21.720(5) Å. The most significant impurity peak is around 28.5°, which is attributed to Bi_2S_3. The experimental and refinement details can be found in the Supporting Information. The refined structural parameters are summarized in Table 1, and the structure is depicted as the inset of Figure 1. Notice that the occupancy of the sulfur site is about 0.92, indicating sulfur vacancies in the sample. The existence of sulfur vacancies is confirmed by both the energy-dispersive X-ray (EDX) spectrometer (giving an atomic ratio Bi:S:Cl = 3.0:1.6:1.0) (Figure S1) and the inductively coupled plasma (ICP, giving an atomic ratio Bi:S:Cl = 3.00:1.98:1.00)

Received: December 27, 2018
Published: February 10, 2019

DOI: 10.1021/jacs.8b13796
J. Am. Chem. Soc. 2019, 141, 3404−3408

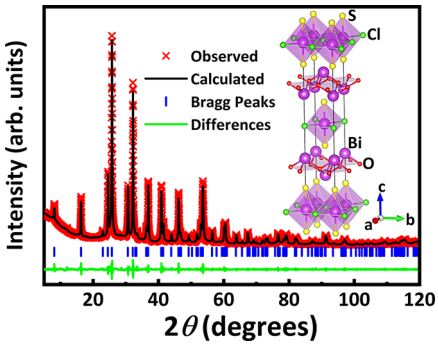

Figure 1. Powder X-ray diffraction pattern of $Bi_3O_2S_2Cl$ with its Rietveld refinement. The inset shows the crystal structure obtained from the refinement, which is drawn with VESTA.[32]

Table 1. Structural Parameters of $Bi_3O_2S_2Cl$ Obtained by Rietveld Refinement[a]

atom	site	x	y	z	occupancy	U_{iso} (Å^2)
Bi1	2a	0	0	0	1.00(3)	0.056(1)
Bi2	4e	0	0	0.3108(1)	0.99(2)	0.024(1)
S	4e	0	0	0.1298(5)	0.92(3)	0.016(2)
O	4d	0.5	0	0.25	1.00(1)	0.012(2)
Cl	2b	0.5	0.5	0	1.00(1)	0.048(3)

[a]Reliability factor R_{wp} = 4.67%.

measurements. The loss of sulfur is probably caused by the residue of Bi_2S_3, as well as the evaporation of sulfur during the synthesizing procedure.

The transmission electron microscopy (TEM) images of different cuts from $Bi_3O_2S_2Cl$ polycrystals are shown in Figure 2 and Figure S2, where the bright spots stand for the positions of large bismuth atoms. The refined positions of the bismuth

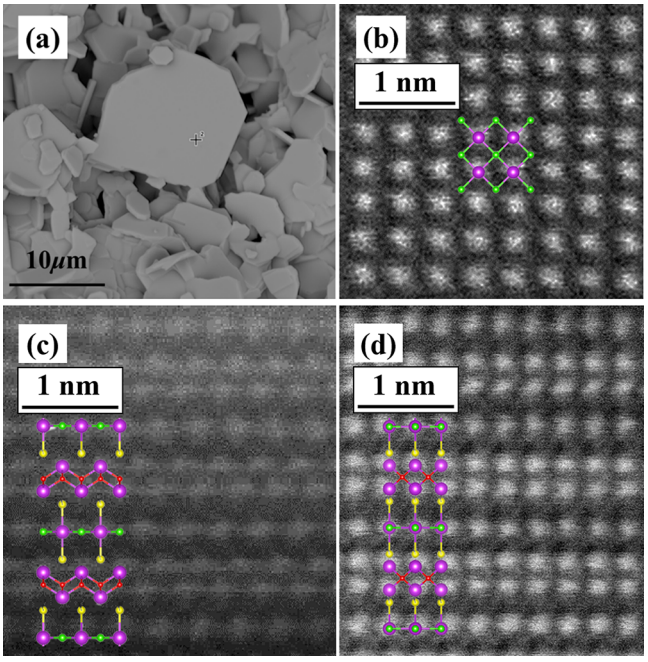

Figure 2. (a) Appearance of the polycrystalline $Bi_3O_2S_2Cl$ under scanning electron microscopy (SEM). (b, c, d) TEM images observed from the directions of [001], [100], and [110], respectively. Insets are the sketches of the refined crystal structure for comparison.

atoms fit well with the TEM images, both of which suggest a novel $[BiS_2Cl]^{2-}$ layer. This structural feature is distinctly different from the $BiCh_2$-based compounds, such as $LaOBiS_2$, $Bi_4O_4S_3$, $Bi_3O_2S_3$, $Eu_3F_4Bi_2S_4$, or $LaO_{1-x}F_xBiSe_2$, all of which consist of $[Bi_2Ch_4]^{2-}$ layers.[6−15,18] Notice that for the $[Bi_2S_4]^{2-}$ layers in $LaOBiS_2$, the in-plane sulfur has the priority to be substituted by selenium.[33] Therefore, it is likely that Cl takes the intralayer sites while S takes the interlayer ones of the $[BiS_2Cl]^{2-}$ layer. This assumption is further backed by the impossibility of mutual doping between S and Cl in our experiments. The geometry optimization and bond valence sum calculation support this assumption too. (see Supporting Information) The unforeseen $[BiS_2Cl]^{2-}$ layer, which is an infinite square planar layer of Bi−Cl decorated with S anions, is unique among the bismuth compounds.

Figure 3a shows the temperature dependence of resistivity for the polycrystalline $Bi_3O_2S_2Cl$ sample under zero magnetic field. The resistivity shows a metallic behavior below 300 K, where a shallow minimum at around 15 K is observed. This pit-like feature of resistivity was also observed in other bismuth sulfides, such as Bi_2S_3 and $K_2Bi_8S_{13}$.[34,35] It results from the freezing of carriers at lower temperatures. Besides, the absolute value of resistivity at 300 K is significantly larger than typical metals, while comparable with those in doped bismuth chalcogenide semiconductors such as $CsBi_4Te_6$, $LaO_{1-x}F_xBiS_2$, or $Sr_{1-x}La_xFBiS_2$.[8,9,36] A drop of resistivity is observed below the superconducting critical temperature T_c (2.6 K), indicating the occurrence of superconductivity. The details of the superconducting transition are demonstrated in Figure 3b. The relatively broad transitions should be attributed to the inhomogeneity of different doping levels in the sample. Various magnetic fields were applied to investigate the superconducting properties. As the magnetic field increases, T_c decreases and the superconducting transition broadens, indicating a suppression of superconductivity by magnetic field. The superconductivity is fully suppressed by a field of 1 T above 1.8 K.

We measured the Hall effects of polycrystalline $Bi_3O_2S_2Cl$ to clarify the carrier's type as well as its concentration in the sample. The measurement was carried out on a thin rectangle cut from the polycrystalline sample. The dimension of the sample was about 8 × 4 × 1 mm. The field dependence of Hall resistivity (ρ_{xy}) was measured at various temperatures from 10 to 275 K. At each temperature, ρ_{xy} was found to be linear with fields up to 4 T, the highest field applied. The field dependences of ρ_{xy} at various temperatures are taken as examples and shown in Figure 3c. The linearity of the Hall effect, which is again distinctly different from that of $LaOBiS_2$, $Bi_4O_4S_3$, and $Bi_3O_2S_3$, suggests a different band structure near the Fermi surface (see Supporting Information).[7,37−39] This difference may arise from the dissimilarity between $[BiS_2Cl]^{2-}$ and $[Bi_2S_4]^{2-}$ layers. Since the Hall coefficient R_H is field independent, it is easily determined by the slope of ρ_{xy} versus $\mu_0 H$. The values of R_H are negative at all temperatures, suggesting that electrons serve as the dominant carriers. The charge carrier concentration is calculated by $n = 1/(eR_H)$, giving 9.34×10^{19} cm^{-3} at 275 K. This value is comparable with that of $Bi_4O_4S_3$ ($\sim 7.28 \times 10^{19}$ cm^{-3} at 300 K), yet much lower than that of typical metals ($\sim 10^{22}$ cm^{-3}).[40] The carrier density corresponds to 0.016 electrons per formula at 275 K, which could be easily introduced by a tiny amount of sulfur vacancies. As shown in Figure 3d, the carrier concentration varies little in the whole temperature range while decreases a

DOI: 10.1021/jacs.8b13796
J. Am. Chem. Soc. 2019, 141, 3404−3408

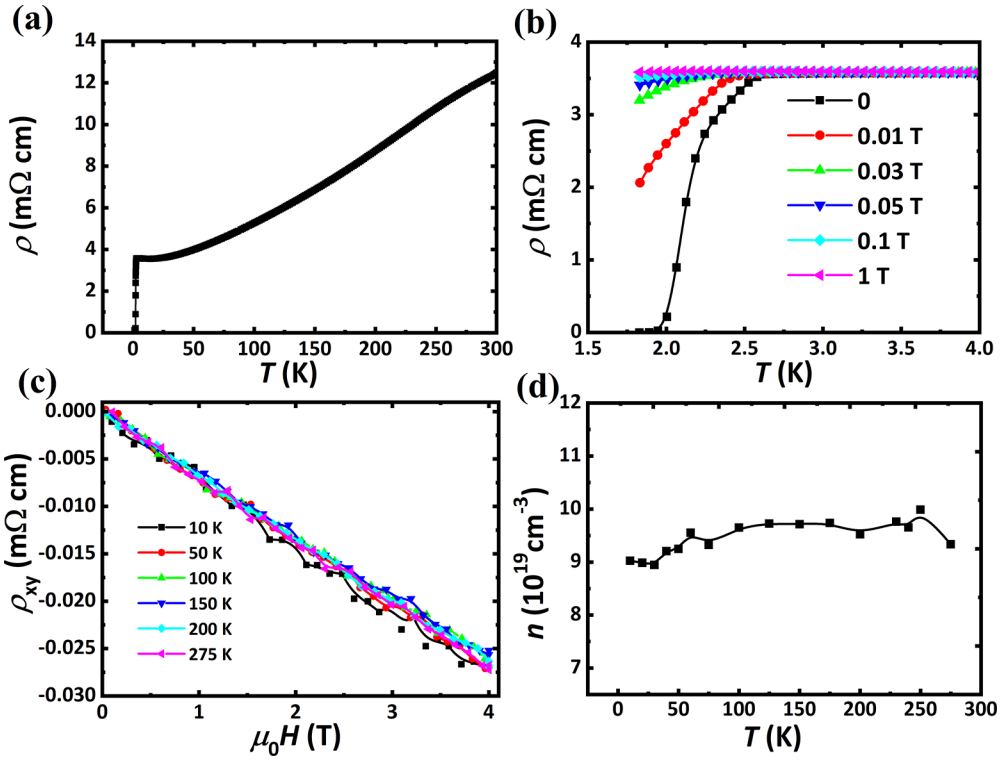

Figure 3. (a) Temperature dependence of resistivity of polycrystalline $Bi_3O_2S_2Cl$. (b) Resistivity under various magnetic fields. (c) Hall resistivity under various temperatures. (d) Carrier concentration calculated from Hall measurement.

little at low temperatures, indicating $Bi_3O_2S_2Cl$ to be a heavily doped semiconductor.

To verify the semiconducting−superconducting transition in $Bi_3O_2S_2Cl$, intentional carrier doping was carried out. We conducted many kinds of doping such as the fluorine substitution of oxygen, the selenium substitution of sulfur, or the doping of element vacancies. Unfortunately, only the doping of sulfur vacancies was successful, which led to changes of the lattice parameters and transport properties. With an increasing of sulfur vacancies, the X-ray diffraction peaks of $Bi_3O_2S_xCl$ shift to higher degrees, indicating a shrinkage of the lattice (Figure S3).

The resistivity of $Bi_3O_2S_xCl$ (x = 2.1, 2.0, 1.95, 1.9) samples with different sulfur contents is shown in Figure 4a, where x stands for the nominal value of the sulfur quantity. Here we successfully obtained the nonsuperconducting sample of the nominal composition of $Bi_3O_2S_{2.1}Cl$, which indeed demonstrated a semiconducting behavior below 100 K. This sample could be considered as the "parent compound" of the $Bi_3O_2S_2Cl$ superconductors. The conductivity of the sample increases with the introduction of sulfur vacancies, and superconductivity of T_c = 3.5 K was also observed. As revealed in Figure 4b, the diamagnetic signals grow larger above 1.8 K. In other words, doping of sulfur vacancies enhances the superconducting phase in the sample, which could also be the origin of superconductivity in the pristine (not intentionally doped) $Bi_3O_2S_2Cl$.

In some batches of the $Bi_3O_2S_2Cl$ polycrystal growth, we were able to collect a few pieces of plate-like single crystals on the sample surfaces, including brownish and transparent ones. XRD measurement reveals the brownish ones to be $Bi_3O_2S_2Cl$, while the transparent ones are BiOCl. The typical size of $Bi_3O_2S_2Cl$ single crystals is about 0.08 × 0.06 × 0.01 mm, as

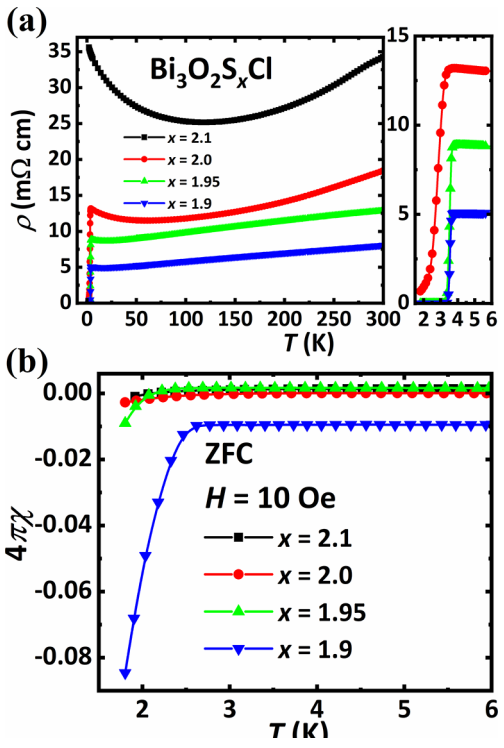

Figure 4. (a) Temperature dependence of resistivity and (b) magnetic susceptibility of the doped samples of nominal compositions of $Bi_3O_2S_xCl$ (x = 2.1, 2.0, 1.95, 1.9).

shown in the inset of Figure 5a. X-ray diffraction of the single crystals only consists of (00l) reflections (l = 2, 4, 6, 8, ...), indicating the surface of the single crystals to be perpendicular to the c-axis. The reflections are also consistent with the body-

DOI: 10.1021/jacs.8b13796
J. Am. Chem. Soc. 2019, 141, 3404−3408

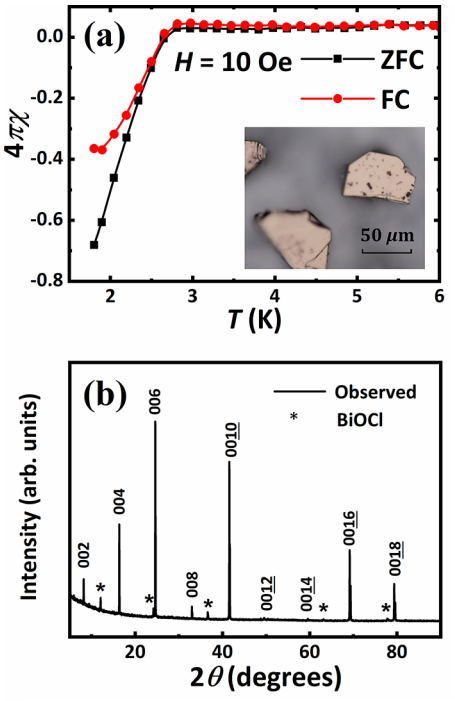

Figure 5. (a) Magnetic susceptibility of $Bi_3O_2S_2Cl$ single crystals. The inset shows the appearance of the single crystals under an optical microscope. (b) X-ray diffraction pattern of the surface of the single crystals. The labeled peaks belong to the $Bi_3O_2S_2Cl$ phase, while small amount of BiOCl is marked with the asterisk.

centered space group of $Bi_3O_2S_2Cl$. According to the (00*l*) peaks, the lattice parameter *c* is calculated to be 21.70 Å, which is slightly smaller than that of the polycrystals. The magnetic susceptibility of the single crystals was measured with magnetic field parallel to the plane of the sample. Superconductivity with a T_c = 2.8 K is also observed in the single-crystalline $Bi_3O_2S_2Cl$ sample. The diamagnetic signals are both significant in the ZFC and the FC runs, verifying the superconductivity. Notice that the diamagnetic signal is much larger than those of the polycrystalline samples above 1.8 K.

The relatively higher growing temperatures (compared to the polycrystalline ones, see Supporting Information) tended to introduce more sulfur vacancies, which resulted in a smaller *c*-axis and consequentially a larger shielding fraction of superconductivity in the single crystals. Carrier doping was realized either by the existence of site vacancies, or by the formation of stacking faults (such as the BiOCl-like stacking faults) caused by the lack of sulfur. Further studies should be carried out to obtain more and larger single crystals to elucidate the electronic consequences of sulfur vacancies therein.

In summary, a new layered compound $Bi_3O_2S_2Cl$ was synthesized via solid-state reactions. As revealed by the Rietveld refinement and TEM images, $Bi_3O_2S_2Cl$ adopts a layered-type structure built with alternatively stacking of $[Bi_2O_2]^{2+}$ and $[BiS_2Cl]^{2-}$ layers. It marks the first compound with the infinite Bi−Cl square-planar layers. Electrical transport measurements reveal $Bi_3O_2S_2Cl$ to be an *n*-type semiconductor, in which superconductivity can be introduced by doping of the sulfur vacancies. The $[BiS_2Cl]^{2-}$ layer is a novel building block in the layered compounds, which provides another option for the search of bismuth materials.

■ ASSOCIATED CONTENT

Supporting Information

The Supporting Information is available free of charge on the ACS Publications website at DOI: 10.1021/jacs.8b13796.

Experimental and calculation details, the energy-dispersive X-ray spectrum of $Bi_3O_2S_2Cl$, powder X-ray diffraction data of the doped samples of $Bi_3O_2S_xCl$ (x = 2.1, 2.0, 1.95, 1.9), and a discussion on the $[BiS_2Cl]^{2-}$ layer (PDF)

Crystallographic information file for $Bi_3O_2S_2Cl$ (CIF)

■ AUTHOR INFORMATION

Corresponding Author

*renzhian@iphy.ac.cn

ORCID

Bin-Bin Ruan: 0000-0003-4642-7782

Zhi-An Ren: 0000-0003-4308-7372

Notes

The authors declare no competing financial interest.

■ ACKNOWLEDGMENTS

This work was supported by the National Natural Science Foundation of China (Grant Nos. 11474339 and 11774402), the National Basic Research Program of China (Grant No. 2016YFA0300301), and the Youth Innovation Promotion Association of the Chinese Academy of Sciences.

■ REFERENCES

(1) Mishra, S. K.; Satpathy, S.; Jepsen, O. Electronic Structure and Thermoelectric Properties of Bismuth Telluride and Bismuth Selenide. *J. Phys.: Condens. Matter* **1997**, *9*, 461.

(2) Venkatasubramanian, R.; Siivola, E.; Colpitts, T.; O'Quinn, B. Thin-film Thermoelectric Devices with High Room-Temperature Figures of Merit. *Nature* **2001**, *413*, 597.

(3) Tang, X. F.; Xie, W. J.; Li, H.; Zhao, W. Y.; Zhang, Q. J.; Niino, M. Preparation and Thermoelectric Transport Properties of High-Performance p-type Bi_2Te_3 with Layered Nanostructure. *Appl. Phys. Lett.* **2007**, *90*, 012102.

(4) Chen, Y. L.; Analytis, J. G.; Chu, J. H.; Liu, Z. K.; Mo, S. K.; Qi, X. L.; Zhang, H. J.; Lu, D. H.; Dai, X.; Fang, Z.; Zhang, S. C.; Fisher, I. R.; Hussain, Z.; Shen, Z. X. Experimental Realization of a Three-Dimensional Topological Insulator, Bi_2Te_3. *Science* **2009**, *325*, 178.

(5) Zhang, Y.; He, K.; Chang, C. Z.; Song, C. L.; Wang, L. L.; Chen, X.; Jia, J. F.; Fang, Z.; Dai, X.; Shan, W. Y.; Shen, S. Q.; Niu, Q.; Qi, X. L.; Zhang, S. C.; Ma, X. C.; Xue, Q. K. Crossover of the Three-Dimensional Topological Insulator Bi_2Se_3 to the Two-Dimensional Limit. *Nat. Phys.* **2010**, *6*, 584.

(6) Mizuguchi, Y.; Fujihisa, H.; Gotoh, Y.; Suzuki, K.; Usui, H.; Kuroki, K.; Demura, S.; Takano, Y.; Izawa, H.; Miura, O. BiS_2-Based Layered Superconductor $Bi_4O_4S_3$. *Phys. Rev. B: Condens. Matter Mater. Phys.* **2012**, *86*, 220510.

(7) Shao, J. F.; Liu, Z. H.; Yao, X.; Pi, L.; Tan, S.; Zhang, C. J.; Zhang, Y. H. Bulk Superconductivity in Single-Phase $Bi_3O_2S_3$. *Phys. Status Solidi RRL* **2014**, *8*, 845.

(8) Mizuguchi, Y.; Demura, S.; Deguchi, K.; Takano, Y.; Fujihisa, H.; Gotoh, Y.; Izawa, H.; Miura, O. Superconductivity in Novel BiS_2-Based Layered Superconductor $LaO_{1-x}F_xBiS_2$. *J. Phys. Soc. Jpn.* **2012**, *81*, 114725.

(9) Lin, X.; Ni, X. X.; Chen, B.; Xu, X. F.; Yang, X. X.; Dai, J. H.; Li, Y. K.; Yang, X. J.; Luo, Y. K.; Tao, Q.; Cao, G. H.; Xu, Z. A. Superconductivity Induced by La Doping in $Sr_{1-x}La_xFBiS_2$. *Phys. Rev. B: Condens. Matter Mater. Phys.* **2013**, *87*, 020504.

(10) Xing, J.; Li, S.; Ding, X. X.; Yang, H.; Wen, H. H. Superconductivity Appears in the Vicinity of Semiconducting-Like

DOI: 10.1021/jacs.8b13796
J. Am. Chem. Soc. 2019, 141, 3404−3408

Behavior in $CeO_{1-x}F_xBiS_2$. *Phys. Rev. B: Condens. Matter Mater. Phys.* **2012**, *86*, 214518.
(11) Jha, R.; Kumar, A.; Singh, S. K.; Awana, V. P. S. Synthesis and Superconductivity of New BiS_2 Based Superconductor $PrO_{0.5}F_{0.5}BiS_2$. *J. Supercond. Novel Magn.* **2013**, *26*, 499.
(12) Jha, R.; Kumar, A.; Singh, S. K.; Awana, V. P. S. Superconductivity at 5 K in $NdO_{0.5}F_{0.5}BiS_2$. *J. Appl. Phys.* **2013**, *113*, 056102.
(13) Yazici, D.; Huang, K.; White, B. D.; Chang, A. H.; Friedman, A. J.; Maple, M. B. Superconductivity of F-Substituted *Ln*$OBiS_2$ (*Ln* = La, Ce, Pr, Nd, Yb) Compounds. *Philos. Mag.* **2013**, *93*, 673.
(14) Yazici, D.; Huang, K.; White, B. D.; Jeon, I.; Burnett, V. W.; Friedman, A. J.; Lum, I. K.; Nallaiyan, M.; Spagna, S.; Maple, M. B. Superconductivity Induced by Electron Doping in $La_{1-x}M_xOBiS_2$ (M = Ti, Zr, Hf, Th). *Phys. Rev. B: Condens. Matter Mater. Phys.* **2013**, *87*, 174512.
(15) Yazici, D.; Jeon, I.; White, B. D.; Maple, M. B. Superconductivity in Layered BiS_2-Based Compounds. *Phys. C* **2015**, *514*, 218.
(16) Lee, P. A.; Nagaosa, N.; Wen, X. G. Doping a Mott Insulator: Physics of High Temperature Superconductivity. *Rev. Mod. Phys.* **2006**, *78*, 17.
(17) Johnston, D. C. The Puzzle of High Temperature Superconductivity in Layered Iron Pnictides and Chalcogenides. *Adv. Phys.* **2010**, *59*, 803.
(18) Zhai, H. F.; Zhang, P.; Wu, S. Q.; He, C. Y.; Tang, Z. T.; Jiang, H.; Sun, Y. L.; Bao, J. K.; Nowik, I.; Felner, I.; Zeng, Y. W.; Li, Y. K.; Xu, X. F.; Tao, Q.; Xu, Z. A.; Cao, G. H. Anomalous Eu Valence State and Superconductivity in Undoped $Eu_3Bi_2S_4F_4$. *J. Am. Chem. Soc.* **2014**, *136*, 15386.
(19) Zhang, K. L.; Liu, C. M.; Huang, F. Q.; Zheng, C.; Wang, W. D. Study of the Electronic Structure and Photocatalytic Activity of the BiOCl Photocatalyst. *Appl. Catal., B* **2006**, *68*, 125.
(20) Li, J.; Yu, Y.; Zhang, L. Z. Bismuth Oxyhalide Nanomaterials: Layered Structures Meet Photocatalysis. *Nanoscale* **2014**, *6*, 8473.
(21) Park, B. W.; Philippe, B.; Zhang, X.; Rensmo, H.; Boschloo, G.; Johansson, E. M. Bismuth Based Hybrid Perovskites $A_3Bi_2I_9$ (A: Methylammonium or Cesium) for Solar Cell Application. *Adv. Mater.* **2015**, *27*, 6806.
(22) Hoye, R. L.; Brandt, R. E.; Osherov, A.; Stevanović, V.; Stranks, S. D.; Wilson, M. W.; Kim, H.; Akey, A. J.; Perkins, J. D.; Kurchin, R.; Poindexter, J. R.; Wang, E. N.; Bawendi, M. G.; Bulović, V.; Buonassisi, T. Methylammonium Bismuth Iodide as a Lead-Free, Stable Hybrid Organic-Inorganic Solar Absorber. *Chem. - Eur. J.* **2016**, *22*, 2605.
(23) Bass, K. K.; Estergreen, L.; Savory, C. N.; Buckeridge, J.; Scanlon, D. O.; Djurovich, P. I.; Bradforth, S. E.; Thompson, M. E.; Melot, B. C. Vibronic Structure in Room Temperature Photoluminescence of the Halide Perovskite $Cs_3Bi_2Br_9$. *Inorg. Chem.* **2017**, *56*, 42.
(24) Friedman, R. M.; Corbett, J. D. Synthesis and Structural Characterization of Bismuth(1+) Nonabismuth(5+) Hexachlorohafnate(IV), $Bi^+Bi_9^{5+}(HfCl_6^{2-})_3$. *Inorg. Chem.* **1973**, *12*, 1134.
(25) Bartl, H. Saving of Measuring Time by Profile Evaluation in the Recording of Neutron Single-Crystal Intensities — Crystal-Structure of $BiCl_3$. *Fresenius' Z. Anal. Chem.* **1982**, *312*, 17.
(26) Hampel, S.; Schmidt, P.; Ruck, M. Synthesis, Thermochemical Properties and Crystal Structure of Bi_7Cl_{10}. *Z. Anorg. Allg. Chem.* **2005**, *631*, 272.
(27) von Benda, H.; Simon, A.; Bauhofer, W. Zur Kenntnis von BiBr und $BiBr_{1.167}$. *Z. Anorg. Allg. Chem.* **1978**, *438*, 53.
(28) von Schnering, H. G.; von Benda, H.; Kalveram, C. Bismuth Monoiodide, a Compound with Bi(0) and Bi(II). *Z. Anorg. Allg. Chem.* **1978**, *438*, 37.
(29) Trotter, J.; Zobel, T. The Crystal Structure of SbI_3 and BiI_3. *Z. Kristallogr. - Cryst. Mater.* **1966**, *123*, 67.
(30) Benachenhou, F.; Mairesse, G.; Nowogrocki, G.; Thomas, D. Structural Studies of Cs-K-Bi Mixed Chlorides Relation to the Crystal Structures of A_2BMX_6, A_3MX_6 and A_2MX_6. *J. Solid State Chem.* **1986**, *65*, 13.
(31) Keramidas, K. G.; Voutsas, G. P.; Rentzeperis, P. I. The Crystal-Structure of BiOCl. *Z. Kristallogr. - Cryst. Mater.* **1993**, *205*, 35.
(32) Momma, K.; Izumi, F. VESTA 3 for Three-Dimensional Visualization of Crystal, Volumetric and Morphology Data. *J. Appl. Crystallogr.* **2011**, *44*, 1272.
(33) Tanaka, M.; Yamaki, T.; Matsushita, Y.; Fujioka, M.; Denholme, S. J.; Yamaguchi, T.; Takeya, H.; Takano, Y. Site Selectivity on Chalcogen Atoms in Superconducting La(O,F)BiSSe. *Appl. Phys. Lett.* **2015**, *106*, 112601.
(34) Kanatzidis, M. G.; McCarthy, T. J.; Tanzer, T. A.; Chen, L. H.; Iordanidis, L.; Hogan, T.; Kannewurf, C. R.; Uher, C.; Chen, B. Synthesis and Thermoelectric Properties of the New Ternary Bismuth Sulfides $KBi_{6.33}S_{10}$ and $K_2Bi_8S_{13}$. *Chem. Mater.* **1996**, *8*, 1465.
(35) Chen, B. X.; Uher, C.; Iordanidis, L.; Kanatzidis, M. G. Transport Properties of Bi_2S_3 and the Ternary Bismuth Sulfides $KBi_{6.33}S_{10}$ and $K_2Bi_8S_{13}$. *Chem. Mater.* **1997**, *9*, 1655.
(36) Malliakas, C. D.; Chung, D. Y.; Claus, H.; Kanatzidis, M. G. Superconductivity in the Narrow-Gap Semiconductor $CsBi_4Te_6$. *J. Am. Chem. Soc.* **2013**, *135*, 14540.
(37) Singh, S. K.; Kumar, A.; Gahtori, B.; Shruti; Sharma, G.; Patnaik, S.; Awana, V. P. S. Bulk Superconductivity in Bismuth Oxysulfide $Bi_4O_4S_3$. *J. Am. Chem. Soc.* **2012**, *134*, 16504.
(38) Tan, S. G.; Li, L. J.; Liu, Y.; Tong, P.; Zhao, B. C.; Lu, W. J.; Sun, Y. P. Superconducting and Thermoelectric Properties of New Layered Superconductor $Bi_4O_4S_3$. *Phys. C* **2012**, *483*, 94.
(39) Mizuguchi, Y.; Omachi, A.; Goto, Y.; Kamihara, Y.; Matoba, M.; Hiroi, T.; Kajitani, J.; Miura, O. Enhancement of Thermoelectric Properties by Se Substitution in Layered Bismuth-Chalcogenide $LaOBiS_{2-x}Se_x$. *J. Appl. Phys.* **2014**, *116*, 163915.
(40) Srivastava, P.; Shruti; Patnaik, S. Structural, Electromagnetic and Thermoelectric Properties of $Bi_4O_4S_3$ superconductor. *Supercond. Sci. Technol.* **2014**, *27*, 055001.

DOI: 10.1021/jacs.8b13796
J. Am. Chem. Soc. 2019, 141, 3404−3408